

Frequency response of graphene phonons to heating and compression

X. X. Yang,¹ J. W. Li,¹ Z. F. Zhou,¹ Y. Wang,² W. T. Zheng,³ and Chang Q. Sun^{1,4,a)}

¹*Institute for Quantum Engineering and Micro-Nano Energy Technology, Key Laboratory of Low-Dimensional Materials and Application Technologies, and Faculty of Materials and Optoelectronic Physics, Xiangtan University, Hunan 411105, China*

²*School of Information and Electronic Engineering, Hunan University of Science and Technology, Xiangtan 411201, China*

³*Department of Materials Science, Jilin University, Changchun 130012, China*

⁴*School of Electrical and Electronic Engineering, Nanyang Technological University, Singapore 639798, Singapore*

(Received 29 August 2011; accepted 7 September 2011; published online 27 September 2011)

The thermally softened and the mechanically stiffened graphene phonons have been formulated from the perspective of bond order-length-strength correlation with confirmation of the C–C bond length in the single-layer graphene contracting from 0.154 to 0.125 nm and the binding energy increasing from 0.65 to 1.04 eV. Matching theory to the measured temperature- and pressure-dependent Raman shift has derived that the Debye temperature drops from 2230 to 540 K, the atomic cohesive energy drops from 7.37 to 3.11 eV/atom, and the binding energy density increases from 250 to 320 eV/nm³ compared with the respective quantities of bulk diamond. © 2011 American Institute of Physics. [doi:10.1063/1.3645015]

Graphene has attracted tremendous interest in recent years because of its extraordinary properties including optical¹ and electrical conductivity,² mechanical strength,³ thermal conductivity,^{4–7} electron emissibility,⁸ the unexpected edge states, and its potential device applications at the nanoscale.^{4,9–11} Overwhelming contributions have been made to explore the lattice dynamics using Raman spectroscopy under various conditions such as temperature (T),^{12–20} pressure (P),²¹ and substrate conditions.²² Generally, the Raman shifts of graphene are softened by heating and stiffened by high-pressure compression. The empirically quadratic and stimuli-parameter apparent functions^{23,24} can reproduce the trends of observations despite the involvement of freely-adjustable parameters, a comprehensive understanding of the phenomena from the perspective of bond relaxation and vibration is still lacking. In fact, the external stimuli such as T and P activate a certain set of intrinsic parameters such as bond length and bond energy that governs the Raman shift intrinsically.²⁵

The objective of this communication is to show that matching the predictions of the bond order-length-strength (BOLS) correlation^{26,27} and local bond average (LBA) approach²⁸ to the Raman spectroscopy has enabled us to reconcile the effects of T and P on the Raman 2D phonon shifts of graphene with consistent insight into the mechanism behind the fascinations and quantitative information of the bond length, bond energy E_b , atomic cohesive energy E_{coh} , binding energy density E_{den} , Debye temperature θ_D , and compressibility β .

The BOLS theory indicates that bonds between under-coordinated (z) atoms become shorter and stronger

$$\begin{cases} d_z/d_b = C_z = 2/\{1 + \exp[(12-z)/8z]\} & (\text{bond contraction}) \\ E_z/E_b = C_z^{-m} & (\text{bond strengthening}) \end{cases} \quad (1)$$

The subscripts z and b denote an atom with z coordination neighbors and in the bulk as a standard, respectively. The bond contraction coefficient C_z varies only with the effective z of the atom of concern regardless of the nature of the bond or the solid dimension. The index $m = 2.56$ is the bond nature indicator of carbon.²⁹ Using the length of 0.154 nm for the C–C bond in diamond and 0.142 nm in graphite, one can readily derive the effective CN for the bulk graphite as $z_g = 5.335$, according to the bond contraction coefficient. For the C atom in the bulk diamond, the effective CN is 12 instead of 4 because the diamond structure is an interlock of two fcc unit cells. Recent progress^{25,26,29,30} confirmed consistently that the C–C bond of the three-coordinated atom in graphene contracts from 0.154 to 0.125 nm. By the relation of $E_z = C_z^{-m} E_b$ and the known atom cohesive energy of diamond, 7.37 eV,³¹ the single C–C bond energy in the diamond is $E_b = 7.37/12 = 0.615$ eV and it is $E_3 = 1.039$ eV in the monolayer graphene of $z = 3$. The cohesive energy in graphene is 3.11 eV/atom. These findings agree well with the fact that³² breaking a 2-coordinated C–C bond requires (7.50 eV per bond) 32% more than that (5.67 eV/bond) for breaking a 3-coordinated C–C bond in a suspended graphene.

Equaling the energy of a vibronic system to the third term in the Taylor series of the interatomic potential, one can derive the phonon frequency shift as a function of the atomic coordination, bond length, bond energy, and the reduced mass of the dimer atoms (z , d_z , E_z , μ) with $\mu = m_1 m_2 / (m_1 + m_2)$

$$\begin{aligned} \Delta\omega(z, P, T) &= \omega(z, P, T) - \omega(0, T_0, P_0) \\ &\propto \frac{z}{d(z, P, T)} \left(\frac{E(z, P, T)}{\mu} \right)^{1/2} \end{aligned}$$

^{a)}Electronic mail: ecqsun@ntu.edu.sg.

With

$$\begin{cases} d(z,P,T) = d_b \left[\left(1 + (C_z - 1)\right) \left(1 + \int_{T_0}^T \alpha(t) dt\right) \left(1 - \int_{P_0}^P \beta(p) dp\right) \right] \\ E(z,P,T) = E_b \left[1 + \frac{(C_z^m - 1) - \int_{T_0}^T \eta(t) dt - \int_{V_0}^V p(v) dv}{E_b} \right] \end{cases} \quad (2)$$

being the z -, T -, and P -dependent bond length and bond energy; T_0 and P_0 are the references at the ambient conditions. For large graphene, the mass μ and z remain constant, and hence, the Raman shift is proportional to the $E^{1/2}/d$ in dimension. The unknown $\omega(0)$ is the reference point from which the Raman shift proceeds. $\alpha(t)$ and $\beta(p)$ are, respectively, the thermal expansion coefficient and the compressibility. $\eta(t)$ is the specific heat of the representative bond. These expressions indicate that the mechanical work hardening by compression will shorten and strengthen but heating will elongate and weaken the C–C bond. From matching to the measurements we can quantify the aforementioned coefficients without involving hypothetical parameters.

For the clarity and convenience, here we focus on the 2D mode that is the secondary term of the solution, in the form of Fourier series, to the Hamiltonian of the vibronic system. The 2D frequency is approximately double that of the primary D term rather than the frequency of two phonons. With the given Raman frequency of the 2D peak shifting from $\omega(z_g = 5.335 \text{ for graphite}) = 2720$ to $\omega(z = 3 \text{ for graphene}) = 2680 \text{ cm}^{-1}$,^{33–35} we can determine the $\omega(0)$ from Eq. (2)

$$\begin{cases} \frac{\omega(3) - \omega(0)}{\omega(z_g) - \omega(0)} = \frac{3}{z_g} \left(\frac{C_z}{C_{z_g}}\right)^{-(2.56/2+1)} = A \\ \omega(0) = \frac{\omega(3) - \omega(z_g)A}{1-A} = 2562.6 (\text{cm}^{-1}) \end{cases}$$

Using the approximation $1 + x \cong \exp(x)$ at $x \ll 1$, we can formulate the thermal and pressure effects³⁶

$$\frac{\omega(z,y) - \omega(0,y_0)}{\omega(z,y_0) - \omega(0,y_0)} \cong \begin{cases} (1 - \Delta_T)^{1/2} \exp\left(\int_{T_0}^T \alpha dt\right) \\ (1 + \Delta_P)^{1/2} \exp\left(\int_{P_0}^P \beta dp\right) \end{cases} \quad (y = T, P) \quad (3)$$

The thermally and mechanically induced energy perturbations Δ_T and Δ_P follow the relations²⁸

$$\begin{aligned} \Delta_T &= \int_{T_0}^T \frac{\eta(t) dt}{E_z} = \int_0^T \frac{C_V(T/\theta_D)}{zE_z} dt \\ &= \int_0^T \frac{4R(T/\theta_D)^2 \int_0^{\theta_D/T} (e^x - 1)^{-1} x^2 dx}{E_{coh}} dt, \\ \Delta_P &= - \int_{V_0}^V \frac{p(v) dv}{E_z} = - \frac{V_0}{E_z} \int_1^x p(x) dx = - \int_1^x \frac{p(x) dx}{E_{den}} \\ x(P) &= V/V_0 = 1 - \beta P + \beta' P^2 \end{aligned} \quad (4)$$

The Δ_T is the integral of the specific heat reduced by the bond energy in two-dimensional Debye approximation. When the measuring temperature T is higher than θ_D , the two-dimensional specific heat C_V approaches a constant of $2R$ (R is the ideal gas constant). The atomic cohesive energy $E_{coh} = zE_z$, and the θ_D are the uniquely adjustable parameters in calculating the Δ_T . The Δ_P is calculated based on the integral of the Birch–Murnaghan (BM) equation,^{37,38} or the nonlinear expression $x(p)$. The V_0 is the initial volume of a bond. The variables in Δ_P are the binding energy density $E_{den} = E_z/V_0$ and the compressibility β and β' . Matching the BM equation to the $x(P)$ curve, one can derive the nonlinear compressibility β and β' . Substituting the integral (4) into (3), we can reproduce the P - and T -dependent Raman shift with derivatives of the θ_D , α , and E_{den} , and the compressibility from the $x(P)$ with the known E_{coh} .

Matching to the measured T -dependent Raman shift of the 2D mode in Fig. 1(a) turns out that $\theta_D = 540 \text{ K}$, with the given atomic cohesive energy of 3.11 eV/atom . The θ_D is about $1/3$ fold of the melting point 1605 K for the single-wall carbon nanotubes (SWNT).²⁹ At $T \sim \theta_D/3$, the Raman shift turns gradually from the nonlinear to the linear form when the temperature is increased. The slow decrease of the Raman shift at very low temperatures arises from the small $\int_0^T \eta dt$ values as the specific heat $\eta(t)$ is proportional to T^2 for the two-dimensional system at very low temperatures. These results imply that the θ_D determines the width of the shoulder; the $1/E_{coh}$ and the α determine the slope of the linear part of the ω - T curve. The match to the measured P -dependent Raman shift in Fig. 1(b) gives rise to the compressibility $\beta = 1.145 \times 10^{-3} (\text{GPa}^{-1})$ and $\beta' = 7.63 \times 10^{-5} (\text{GPa}^{-2})$ and the energy density $E_{den} = 320 \text{ eV/nm}^3$. As we considered the relative Raman shift,²² the substrate effect on the phonon frequency²² does not affect the quantification and the conclusion. The substrate effect may influence the value of the reference $\omega_x(0, T_0, P_0)$ in Eq. (1).

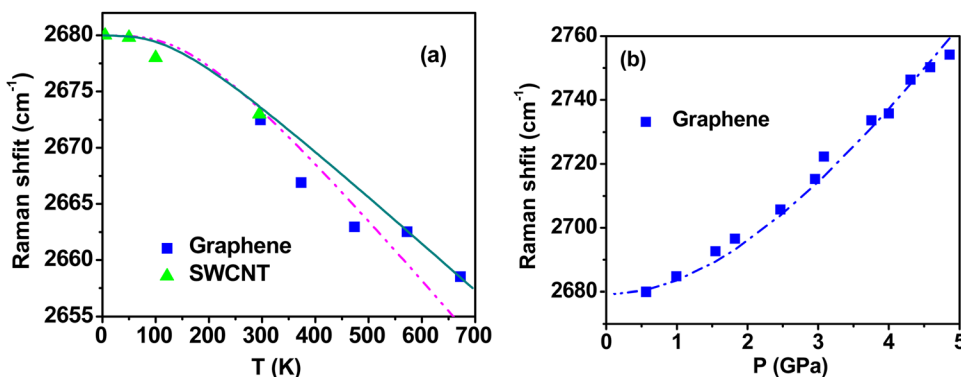


FIG. 1. (Color online) BOLS reproduction of the measured (a) temperature [Refs. 12 and 18] and (b) pressure [Ref. 21] dependent Raman shift of the 2D mode of graphene and SWCNT with derived information as given in Table I.

TABLE I. Instrumental information derived from the reproduction of the T- and P- dependent Raman shift of monolayer graphene.

Stimuli	Quantities	Graphene	Diamond
Temperature	E_{coh} (eV/atom)	3.11	7.37 ^a
	θ_D (K)	540 ($T_m = 1605$) ^b	2230 ^c
	α (10^{-6} K^{-1})	9.0	0.8 ^d
Pressure	E_{den} (eV/nm ³)	320	249.59
	β/β' ($10^{-3} \text{ GPa}^{-1}/\text{GPa}^{-2}$)	1.145/0.0763	2.120/0.0035
	B_0/B'_0 (GPa/–)	690/5 (704/1) ^e	446/3.6 ^f

^aReference 31.^bReference 29.^cReference 39.^dReference 40.^eReference 41.^fReference 42.

Hence, an extension of the BOLS correlation has enabled us to formulate and quantify the T- and P-dependent Raman shift of graphene with clarification of the bonding origin. Quantitative information, as summarized in Table I has been derived regarding the bond length, bond energy, atomic cohesive energy, binding energy density, Debye temperature, and compressibility of graphene in comparison to the respective quantities for bulk diamond. These findings evidence not only the validity of the BOLS correlation in revealing the physical origin of the Raman shift but also the enhanced power of the Raman spectroscopy in quantifying the information.

Financial supports from NSF (Nos. 50832001 and 11172254) of China are gratefully acknowledged.

¹P. Blake, P. D. Brimicombe, R. R. Nair, T. J. Booth, D. Jiang, F. Schedin, L. A. Ponomarenko, S. V. Morozov, H. F. Gleeson, E. W. Hill, A. K. Geim, and K. S. Novoselov, *Nano Lett.* **8**(6), 1704 (2008).

²Y. W. Tan, Y. Zhang, H. L. Stormer, and P. Kim, *Eur. Phys. J.–Spec. Top.* **148**(1), 15 (2007).

³F. Hao, D. N. Fang, and Z. P. Xu, *Appl. Phys. Lett.* **99**(4), 041901 (2011).

⁴S. Ghosh, I. Calizo, D. Teweldebrhan, E. P. Pokatilov, D. L. Nika, A. A. Balandin, W. Bao, F. Miao, and C. N. Lau, *Appl. Phys. Lett.* **92**(15), 151911 (2008).

⁵D. L. Nika, E. P. Pokatilov, A. S. Askerov, and A. A. Balandin, *Phys. Rev. B* **79**(15), 155413 (2009).

⁶A. A. Balandin, *Nature Mater.* **10**(8), 569 (2011).

⁷D. L. Nika, S. Ghosh, E. P. Pokatilov, and A. A. Balandin, *Appl. Phys. Lett.* **94**, 203103 (2009).

⁸I. Childres, L. A. Jauregui, M. Foxe, J. F. Tian, R. Jalilian, I. Jovanovic, and Y. P. Chen, *Appl. Phys. Lett.* **97**(17), 173109 (2010).

⁹C.-C. Lin, D.-Y. Wang, K.-H. Tu, Y.-T. Jiang, M.-H. Hsieh, C.-C. Chen, and C.-W. Chen, *Appl. Phys. Lett.* **98**(26), 263509 (2011).

¹⁰T. V. Cuong, V. H. Pham, E. W. Shin, J. S. Chung, S. H. Hur, E. J. Kim, Q. T. Tran, H. H. Nguyen, and P. A. Kohl, *Appl. Phys. Lett.* **99**(4), 041905 (2011).

¹¹J. C. Meyer, A. K. Geim, M. I. Katsnelson, K. S. Novoselov, T. J. Booth, and S. Roth, *Nature* **446**(7131), 60 (2007).

¹²L. Zhang, Z. Jia, L. M. Huang, S. O'Brien, and Z. H. Yu, *J. Chem. Phys. C* **112**(36), 13893 (2008).

¹³I. Calizo, F. Miao, W. Bao, C. N. Lau, and A. A. Balandin, *Appl. Phys. Lett.* **91**(7), 071913 (2007).

¹⁴K. T. Nguyen, D. Abdula, C.-L. Tsai, and M. Shim, *ACS Nano* **5**(6), 5273 (2011).

¹⁵D. J. Late, U. Maitra, L. S. Panchakarla, U. V. Waghmare, and C. N. R. Rao, *J. Phys.: Condens. Matter* **23**(5), 055303 (2011).

¹⁶D. Abdula, T. Ozel, K. Kang, D. G. Cahill, and M. Shim, *J. Phys. Chem. C* **112**(51), 20131 (2008).

¹⁷M. J. Allen, J. D. Fowler, V. C. Tung, Y. Yang, B. H. Weiller, and R. B. Kaner, *Appl. Phys. Lett.* **93**(19), 193119 (2008).

¹⁸I. Calizo, A. A. Balandin, W. Bao, F. Miao, and C. N. Lau, *Nano Lett.* **7**(9), 2645 (2007).

¹⁹H. Q. Zhou, C. Y. Qiu, F. Yu, H. C. Yang, M. J. Chen, L. J. Hu, Y. J. Guo, and L. F. Sun, *J. Phys. D–Appl. Phys.* **44**(18), 185404 (2011).

²⁰H. Q. Zhou, C. Y. Qiu, H. C. Yang, F. Yu, M. J. Chen, L. J. Hu, Y. J. Guo, and L. F. Sun, *Chem. Phys. Lett.* **501**(4–6), 475 (2011).

²¹J. E. Proctor, E. Gregoryanz, K. S. Novoselov, M. Lotya, J. N. Coleman, and M. P. Halsall, *Phys. Rev. B* **80**(7), 073408 (2009).

²²I. Calizo, W. Bao, F. Miao, C. N. Lau, and A. A. Balandin, *Appl. Phys. Lett.* **91**, 201904 (2007).

²³R. Cusco, E. A. Llado, J. Ibanez, L. Artus, J. Jimenez, B. Wang, and M. J. Callahan, *Phys. Rev. B* **75**(16), 165202 (2007).

²⁴J. Liu and Y. K. Vohra, *Phys. Rev. Lett.* **72**(26), 4105 (1994).

²⁵W. T. Zheng and C. Q. Sun, *Energy & Environ. Sci.* **4**(3), 627 (2011).

²⁶C. Q. Sun, Y. Sun, Y. G. Nie, Y. Wang, J. S. Pan, G. Ouyang, L. K. Pan, and Z. Sun, *J. Chem. Phys. C* **113**(37), 16464 (2009).

²⁷C. Q. Sun, *Prog. Solid State Chem.* **35**(1), 1 (2007).

²⁸C. Q. Sun, *Prog. Mater. Sci.* **54**(2), 179 (2009).

²⁹C. Q. Sun, H. L. Bai, B. K. Tay, S. Li, and E. Y. Jiang, *J. Phys. Chem. B* **107**(31), 7544 (2003).

³⁰X. Zhang, W. T. Zheng, J. L. Kuo, and C. Q. Sun, *Carbon* **49**, 3615 (2011).

³¹C. Kittel, *Introduction to Solid State Physics*, 8 ed. (Wiley, New York, 2005).

³²C. Girit, J. C. Meyer, R. Erni, M. D. Rossell, C. Kisielowski, L. Yang, C. H. Park, M. F. Crommie, M. L. Cohen, S. G. Louie, and A. Zettl, *Science* **323**(5922), 1705 (2009).

³³D. Graf, F. Molitor, K. Ensslin, C. Stampfer, A. Jungen, C. Hierold, and L. Wirtz, *Nano Lett.* **7**(2), 238 (2007).

³⁴A. K. Gupta, T. J. Russin, H. R. Gutierrez, and P. C. Eklund, *ACS Nano* **3**(1), 45 (2008).

³⁵C. Thomsen and S. Reich, *Phys. Rev. Lett.* **85**(24), 5214 (2000).

³⁶M. X. Gu, L. K. Pan, T. C. Au Yeung, B. K. Tay, and C. Q. Sun, *J. Phys. Chem. C* **111**(36), 13606 (2007).

³⁷F. Birch, *Phys. Rev.* **71**(11), 809 (1947).

³⁸F. D. Murnaghan, *Proc. Natl. Acad. Sci. U.S.A.* **30**(9), 244 (1944).

³⁹W. R. Panero and R. Jeanloz, *J. Appl. Phys.* **91**(5), 2769 (2002).

⁴⁰R. Kalish, *Appl. Surf. Sci.* **117–118**, 558 (1997).

⁴¹S. Reich, C. Thomsen, and P. Ordejon, *Phys. Rev. B* **65**(15), 153407 (2002).

⁴²D. L. Farber, J. Badro, C. M. Aracne, D. M. Teter, M. Hanfland, B. Canny, and B. Couzinet, *Phys. Rev. Lett.* **93**(9), 095502 (2004).